Veterinary Pathology
2014, Vol. 51(4) 737-748

DOI: 10.1177/0300985813503568
vet.sagepub.com

Immunohistochemical Vascular Factor Expression in Canine Inflammatory Mammary Carcinoma

L. Camacho[1], L. Peña[2], A. González Gil[1], A. Martín-Ruiz[1], S. Dunner[3], and J. C. Illera[1]

Abstract

Human inflammatory breast carcinoma (IBC) and canine inflammatory mammary carcinoma (IMC) are considered the most malignant types of breast cancer. IMC has similar characteristics to IBC; hence, IMC has been suggested as a model to study the human disease. To compare the angiogenic and angioinvasive features of IMC with non-IMC, 3 canine mammary tumor xenograft models in female SCID mice were developed: IMC, comedocarcinoma, and osteosarcoma. Histopathological and immunohistochemical characterization of both primary canine tumors and xenografts using cellular markers pancytokeratin, cytokeratin 14, vimentin, and α-smooth muscle actin and vascular factors (VEGF-A, VEGF-D, VEGFR-3, and COX-2) was performed. Tumor cell proliferation index was measured by the Ki-67 marker. The xenograft models reproduced histological features found in the primary canine tumor and preserved the original immunophenotype. IMC xenografts showed a high invasive character with tumor emboli in the dermis, edema, and occasional observations of ulceration. In addition, compared with osteosarcoma and comedocarcinoma, the IMC model showed the highest vascular factor expression associated with a high proliferation index. Likewise, IMC xenografts showed higher COX-2 expression associated with VEGF-D and VEGFR-3, as well as a higher presence of dermal lymphatic tumor emboli, suggesting COX-2 participation in IMC lymphangiogenesis. These results provide additional evidence to consider vascular factors, their receptors, and COX-2 as therapeutic targets for IBC.

Keywords

canine mammary tumor, COX-2, immunohistochemistry, inflammatory breast cancer, SCID mice, vascular factors, xenograft

Human inflammatory breast carcinoma (IBC) and canine inflammatory mammary carcinoma (IMC) are considered the most malignant types of breast cancer, showing the worst prognosis in both humans and dogs.[36,48,49] Spontaneous IMC has similar characteristics to IBC; hence, IMC has been suggested as a model to study the human disease.[33,36] Human mammary comedocarcinoma is the ductal carcinoma in situ with the worst prognosis and the highest proliferation rate.[27,46] Yet, little is known about canine mammary comedocarcinoma, considering that it has been included in the most recent classification for canine mammary tumors.[17] Mammary osteosarcoma is a fast-growing and aggressive tumor,[24] and it is the most common mesenchymal neoplasm of the canine mammary gland.[17]

One of the main characteristics of IBC is its high angiogenic and angioinvasive potential, features that contribute to its aggressive behavior.[23] This neoplasm shows marked lymphatic invasion, particularly in the dermis.[23,36] In addition, IBC has increased vascular density, a high rate of endothelial cell proliferation, and high levels of angiogenic and lymphangiogenic factors and receptors in both IMC and IBC compared with other nonmalignant mammary/breast tumors.[8,9,44,53] Therefore, vascular endothelial growth factors (VEGFs) and their receptors have been proposed as therapeutic targets for this disease.[18] It has been observed that vasculogenic mimicry (VM), a process by which highly aggressive tumors can obtain nutrients by themselves in the absence of the classical vessels,[26] is more frequent in IMC/IBC than in any other mammary/breast tumors.[7,45]

Cyclooxygenase-2 (COX-2) plays a role in many breast tumor processes, such as invasion, angiogenesis by increasing the production of VEGFs, or formation of VM.[3,5,10,37] Significant correlations have been found in human breast cancer between COX-2 and angiogenic factors such as VEGF-A,[10] as well as

[1] Department of Animal Physiology, Veterinary Medicine School, Complutense University of Madrid, Madrid, Spain
[2] Department of Animal Medicine, Surgery and Pathology, Veterinary Medicine School, Complutense University of Madrid, Madrid, Spain
[3] Department of Animal Production, Veterinary School, Complutense University of Madrid, Madrid, Spain

Corresponding Author:
L. Camacho Soguero, Dpto. Fisiología (Fisiología Animal), Facultad de Veterinaria, Universidad Complutense de Madrid, Avda. Puerta de Hierro s/n. 28040 Madrid (Spain).
Email: laura_mond@hotmail.com

lymphangiogenic factors such as VEGF-C.[51] In canine mammary tumors, higher concentrations of COX-2 have been observed in IMC compared with other tumors.[8,38] Furthermore, in canine malignant non-IMC mammary tumors, COX-2 immunoexpression was significantly associated with VEGF-A, while in IMC, it was associated with VEGF-D, a lymphangiogenic factor; its receptor, VEGFR-3; and the lymphatic proliferation index, suggesting a specific role of COX-2 in IMC angiogenesis by stimulating the lymphangiogenic pathway.[8] Mouse modeling of human breast cancer is of great value in cancer research. New models have provided a deeper understanding of the fundamental events that mediate the initiation, development, and progression of the disease, as well as novel targets for future interventions in the diagnosis, treatment, and prevention. Therefore, the aim of the present study was to develop 3 canine mammary tumor xenograft models in female SCID mice, 1 IMC and 2 highly malignant non-IMC tumors, to compare the angiogenic and angioinvasive features between them. Histopathological and immunohistochemical characterization of both primary canine tumors and xenografts using cellular markers pancytokeratin (AE1/AE3), cytokeratin 14 (CK14), vimentin, and α–smooth muscle actin was performed. The levels of VEGF-A, VEGF-D, VEGFR-3, COX-2, and the tumor cell proliferation index (Ki-67 marker) were measured comparatively.

Materials and Methods

Animals and Xenograft Establishment

Seventy-two female SCID mice (BALB/cJHan^{TM}Hsd-Prkdc^{SCID}; Harlan Laboratories Models, SL, Barcelona, Spain) were used. The animals were housed in a flexible-film isolator (Isotec; Harlan Laboratories Models, SL) in cages (2–3 animals per cage), each measuring 28 × 12 × 12 cm, in a room with controlled environmental conditions (20–22°C, 50%–55% relative humidity, 10–15 air changes per hour, and a 12:12-hour light/dark cycle). Food and water, previously sterilized, were provided ad libitum. All experimental procedures were performed between 10 AM and 1 PM. Comedocarcinoma and osteosarcoma tumors were selected as highly malignant non-IMC canine mammary tumors since they showed an elevated aggressiveness and poor prognosis in female dogs, which was further confirmed histologically in the primary canine tumors.

The first xenograft was directly established from an 11-year-old female Cocker Spaniel mammary comedocarcinoma. The second xenograft was developed from an 11-year-old female Belgian Shepherd mammary osteosarcoma. Finally, the third xenograft corresponded to an IMC established from an 11-year-old female German Shepherd.

Fragments of 5 × 2–mm tissue were placed in minimum essential medium (MEM) liquid with Earle's salts, L-glutamine, and penicillin/streptomycin (100×; pAA Laboratories, Linz, Austria) immediately after the surgery or necropsy and were subcutaneously implanted into the ventral side of 3 female SCID mice. Animals were previously anesthetized with isoflurane (IsoVet 1000 mg/g; B Braun VetCare SA, Barcelona, Spain) at 4% for induction and 1.5% for maintaining sedation, supplied in a fresh gas flow rate of 0.5 liters of oxygen/minute. Other fragments of tissue were fixed in neutral formalin and paraffin embedded for tumor histology and immunohistochemistry. The samples were histologically diagnosed on hematoxylin and eosin (HE)–stained sections following the most recent histological classification of canine mammary tumors.[17]

When implanted tumors reached approximately 2 cm in diameter, they were twice successively transplanted into 3 SCID mice to verify that the xenograft model was stable and tumors did not change histologically between the 3 consecutive passages. Tumors from the third passage were transplanted into 15 mice per xenograft model. Mice were sacrificed in groups of 3 at 5 consecutive time points to obtain samples at 5 different stages of tumor development. A total of 24 mice per xenograft model were finally transplanted (first 3 passages, n = 9 and final transplants, n = 15), although the histopathological and immunohistochemical studies were developed in 19 comedocarcinoma and osteosarcoma xenografts and in all 24 IMC xenografts. All experimental protocols were approved by the Institutional Animal Care and Use Committee of the Veterinary Faculty at the Universidad Complutense of Madrid, Spain, under the 7.12.2007 Ethical Committee approval. All procedures were completed in accordance with the Guide for the Care and Use of Laboratory Animals and conformed to the relevant European Union directive.

DNA Profiling

A 1-mg sample from each xenograft was used to extract DNA, following a standard phenol-chloroform procedure.[42] The obtained DNA was subjected to amplification of a sequence encoding the ribosomal RNA (rRNA) 12S fraction of the mitochondrial genome using universal primers (Mit12S-FW: CAAACTGGGATTAGAT ACC and Mit12S-RV: TAGAACAGGCTCCTCTAG). The sequences described in GenBank used to perform alignment with the sequences obtained were the *Mus musculus* mitochondrion 12S rRNA gene (NC_005089) and the *Canis familiaris* mitochondrial 12S rRNA gene (Y08507).

Histopathology and Immunohistochemistry

Primary canine tumors and xenografts were characterized by histopathological and immunohistochemical studies using the cellular markers pancytokeratin (CK), CK14, vimentin, and α–smooth muscle actin. The tumor proliferation index was determined by the Ki-67 marker. Immunoexpression of factors related to tumor vascularization, including VEGF-A, VEGF-D, VEGFR-3, and COX-2, was also measured. Endothelial marker CD31 was used to identify vasculogenic mimicry areas. Caspase immunostaining to analyze the presence of apoptotic bodies in the comedocarcinoma xenograft was performed. Immunohistochemistry was performed on deparaffinized sections using the streptavidin-biotin-complex peroxidase method.[22] High-temperature antigen retrieval (HTAR) with 10 mM citrate buffer (pH 6.0) was used for

Table 1. Technical Data of Specific Antibodies.

Primary Antibody	Type	Source	Incubation	Secondary Antibody	Source	Incubation
Pancytokeratin clone AE1/AE3	Mab	Master Diagnostica Prediluted	Overnight 4°C	Horse anti–mouse BA-2000	Vector Laboratories 1:400	30 min, room temperature
Cytokeratin 14 clone LL02	Mab	AbD Serotec 1:1000	Overnight 4°C	Horse anti–mouse BA-2000	Vector Laboratories 1:400	30 min, room temperature
Vimentin clone V9	Mab	Dako 1:1000	ARK kit	ARK kit	ARK kit	ARK kit
Smooth muscle actin clone 1A4	Mab	Master Diagnostica 1:2	ARK kit	ARK kit	ARK kit	ARK kit
Ki-67 clone MIB-1	Mab	Dako 1:25	ARK kit	ARK kit	ARK kit	ARK kit
VEGF-A A-20	Pab	Santa Cruz Biotechnology 1:500	Overnight 4°C	Swine anti–rabbit E0353	Dako 1:200	30 min, room temperature
VEGF-D H-144	Pab	Santa Cruz Biotechnology 1:200	Overnight 4°C	Goat anti–rabbit E0432	Dako 1:300	30 min, room temperature
VEGFR-3 FLT-4 IgG 1	Pab	Alpha Diagnostic International 1:200	Overnight 4°C	Goat multilink MAD-001828QK	Master Diagnostica Prediluted	10 min, room temperature
COX-2 N-20	Pab	Santa Cruz Biotechnology 1:150	Overnight 4°C	Mouse anti–goat N31732	Immunopure 1:1000	30 min, room temperature
CD3 1 clone JC70A	Mab	Dako 1:900	Overnight 4°C	Goat multilink MAD-001828QK	Master Diagnostica Prediluted	10 min, room temperature
Caspase 3	Pab	R&D Systems 1:1000	Overnight 4°C	Swine anti–rabbit E0353	Dako 1:200	30 min, room temperature

Abbreviations: Mab, mouse monoclonal antibody; Pab, rabbit polyclonal antibody.

unmasking the antigen. For VEGFR-3, it was also necessary to use an enzymatic treatment with trypsin 0.01% (Sigma, St Louis, MO) for 10 minutes at 37°C. After incubation with the primary antibodies, the slides were washed and incubated with biotinylated secondary antibody (Table 1). Next, all the slides were incubated with streptavidin conjugated with peroxidase (code 43-4323, 1:400; Zymed, San Francisco, CA) for 30 minutes at room temperature. All washes and dilutions were made in Tris-buffered saline (pH 7.4). All slides were developed with a chromogen solution containing 3,3′-diaminobenzidine tetrachloride (DAB Peroxidase Substrate Kit; Vector Laboratories, Burlingame, CA) and counterstained in hematoxylin (code GH5-2-16; Sigma). Corresponding negative control slides were made by replacing the primary antibody with Tris-buffered saline. Positive controls were also used. Immunostaining for vimentin, α–smooth muscle actin, and Ki-67 marker was done by the ARK kit (code K3954; Dako, Glostrup, Denmark). Tumors were considered positive for CK, vimentin, and actin when more than 50% of the neoplastic cells were positive and positive for CK14 when more than 10% of cells stained. The intensity of immunoexpression was classified as low (+), moderate (++), or intense (+++). The Ki-67 index was calculated as the mean of the proportion of positive nuclei in 8 to 10 representative fields. The presence or absence of VEGF-A, VEGF-D, VEGFR-3, and COX-2 staining was observed in the cytoplasm of the tumor cells. VEGF-A, VEGF-D, and VEGFR-3 immunoreactions were scored in each case as negative (0) or positive (1, low positivity; 2, moderate positivity; and 3, intense positivity). Due to the heterogeneity of the COX-2 inmunostaining, the scoring method was based on the percentage of immunostained cells in combination with the labeling intensity: 0, negative, no staining; 1, low positivity, with weak diffuse staining in 75% to 100% of tumor cells and possible stronger intensity in less than 10% of cells; 2, moderate positivity, with moderate staining in 50% to 100% of tumor cells, with either weak diffuse staining in 75% to 100% of cells and groups of cells (10%–50%) with strong staining or only strong staining in 10% to 50% of tumor cells; and 3, intense positivity, with strong staining in more than 50% of tumor cells. Caspase 3 and CD31 immunostaining were assessed by positive or negative immunoexpression in neoplastic cells.

Statistical Analysis

Statistical analysis was performed by the SPSS version 19.0 for Windows (SPSS< Inc, an IBMM Company, Chicago, IL). The relationship between continuous and categorical variables was performed using analysis of variance followed by appropriate post hoc tests for similar (Duncan test) or different (Games-Howell test) variances. The relationship between continuous variables was assessed using Pearson correlation. The association between categorical variables was analyzed using Pearson's χ^2 test. Differences were considered significant at $P < .05$.

Results

Three stable serial transplantable xenografts were successfully established (Fig. 1–6). No significant differences were found between the 5 time points of tumor development in any of the studied factors.

DNA Profile

The resulting amplified ribosomal RNA sequence for all 3 tumor models was GCAATAGCTTAAAACTCAAAG-GACTTGGCGGTGCTTTATATCCCTCTAGAGGAGCCTG

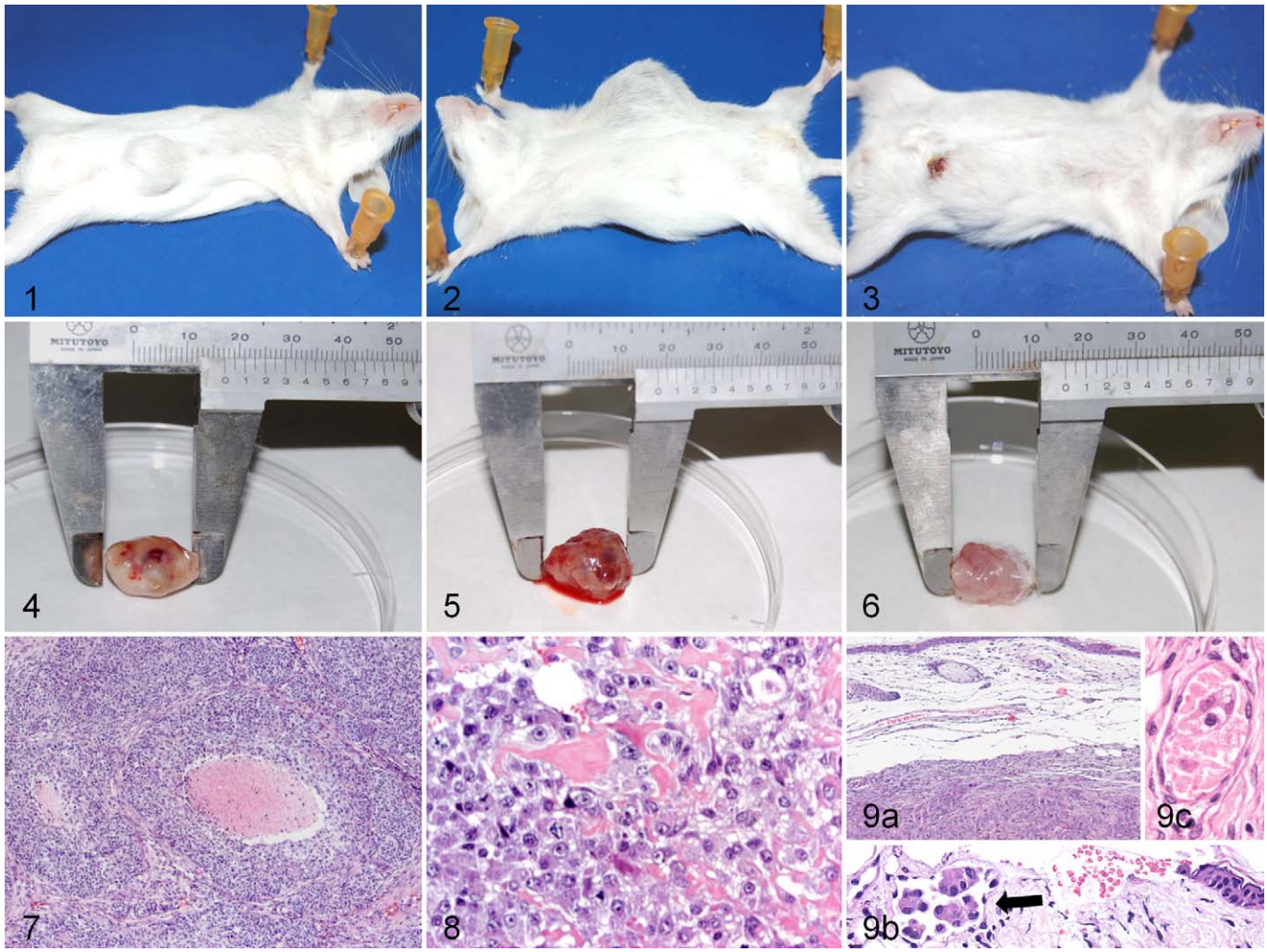

Figure 1. Adult SCID (BALB/cJHan^{TM}Hsd-Prkdc^{SCID}) mouse No. 1. Mammary comedocarcinoma (CC) xenograft appearance at the site of subcutaneous (SC) inoculation. **Figure 2.** Adult SCID mouse No. 2. Mammary osteosarcoma (OS) xenograft appearance at the site of SC inoculation. **Figure 3.** Adult SCID mouse No. 3. Inflammatory mammary carcinoma (IC) xenograft appearance at the site of SC inoculation. **Figure 4.** Mammary CC tumor; SCID mouse xenograft No. 1. Gross appearance of the CC xenograft. **Figure 5.** Mammary OS tumor; SCID mouse xenograft No. 2. Gross appearance of the OS xenograft. **Figure 6.** Mammary IC tumor; SCID mouse xenograft No. 3. Gross appearance of the IC xenograft. **Figure 7.** Mammary CC tumor; SCID mouse xenograft No. 1. Histological appearance of comedo structures formed by neoplastic cell aggregates surrounding necrotic areas. Hematoxylin and eosin (HE). **Figure 8.** Mammary OS tumor; SCID mouse xenograft No. 2. Histological appearance of mammary osteosarcoma with osteoid matrix. HE. **Figure 9.** Mammary IC tumor; SCID mouse xenograft No. 3. Histological appearance: (a) IC tumor showing marked edema. HE. (b) Arrow showing tumor embolus in dermis. HE. (c) Skin; endothelial-like cells (vasculogenic mimicry) forming a neoplastic embolus in the dermal blood capillary. Note the presence of a leukocyte inside the VM channel. HE.

TTCTA, identical to the sequence described in GenBank for the canine species, proving that the genetic content of the xenografts was entirely canine.

Histopathologic Study in Canine Original Tumor and Xenografts

The first model was histopathologically diagnosed as comedotype solid mammary carcinoma (CC). Large polygonal to pleomorphic epithelial cells with nondefined cytoplasmic limits and some myoepithelial cells were observed. Some groups of solid cells showed a necrotic center (comedo), in which karyorrhexis and apoptotic bodies were identified. Xenografts reproduced the histological features from the primary canine tumor (Fig. 7). The second model was diagnosed as canine mammary osteosarcoma (OS). As in the primary tumor, the osteoid matrix was identified in xenografts (Fig. 8), and the cells were markedly pleomorphic, showing anisokaryosis and atypical mitoses. The third primary tumor was diagnosed as inflammatory tubular solid carcinoma (IC), while some xenografts were diagnosed as tubular and some as solid carcinomas. All IC xenografts were histologically categorized as grade III. They showed marked edema (Fig. 9a) and occasionally produced ulceration (12.5%). Similar to the original tumor,

Table 2. Immunohistochemical Characterization of Tumor Phenotype.

	Comedocarcinoma		Osteosarcoma		Inflammatory Carcinoma	
Factor	Canine Tumor	Xenografts	Canine Tumor	Xenografts	Canine Tumor	Xenografts
AE1/AE3 (pancytokeratin)	3	2 (6.6) 3 (93.3)	0	0 (100)	3	3 (100)
Cytokeratin 14	2	1 (60.0) 2 (40.0)	0	0 (100)	2	1 (16.7) 2 (83.3)
Vimentin	2	0 (15.8) 1 (52.6) 2 (31.6)	2	1 (15.8) 2 (84.2)	1	1 (62.5) 2 (37.5)
Actin	2	1 (10.5) 2 (89.5)	0	0 (100)	0	0 (100)

Immunoexpression was classified in categories from 0 to 3 based on the amount of positive cells and the staining intensity. In xenografts, the percentage of tumors corresponding to this intensity is shown in parentheses.

xenografts were composed of large and highly pleomorphic cells with clearly defined limits, marked cytoplasmic atypia and anisokaryosis, clumped chromatin, 1 to 2 nucleoli, a high mitotic index, and atypical mitosis. The stroma was scant (66.6%) or moderate (33.3%), with desmoplasia in 3 cases (12.5%). Tumors showed a highly invasive character with tumor emboli in the dermis (Fig. 9b) and in other tumor areas (33.3% and 25%, respectively). Necrotic tumor cells were identified in the emboli in 3 cases. Lymphangiectasia and vasculogenic mimicry (Fig. 9c) were frequently identified (81% and 66.7%, respectively). Negative staining for endothelial marker CD31 in vasculogenic mimicry areas confirmed the cells were not endothelial in origin. Necrotic areas (87.5%) and pyknotic cells (95.8%) were frequent.

Immunohistochemical Characterization of Tumor Phenotype

Factor expression for characterization of tumor phenotype is summarized in Table 2. For pancytokeratin, both the original tumor and xenografts (93.3%) were slightly positive (+) for AE1/AE3 in comedocarcinoma. Strongly positive (+++) cells, isolated or in small groups, with heterogeneous distribution were also found (Fig. 10a). Both canine and xenograft cells were negative in osteosarcoma (Fig. 11a). However, both the original tumor and xenografts in IC were strongly positive (+++), and some positive cells were found in dermal emboli (Fig. 12a). In CC, 80% of canine tumor cells and 10% to 30% of xenograft cells were positive (moderate to strong) for CK14 (Fig. 10b). In many cases, these groups of cells were distributed in comedo formations. The OS model was negative for this marker (Fig. 11b), but both canine and xenografts (83.3%) showed a moderate positivity in IC (Fig. 12b). For vimentin, both the canine tumors and xenografts in all 3 models showed a light to moderate expression (Figs. 10c, 11c, 12c). For smooth muscle actin, while CC showed moderate or intense positivity (Fig. 10d), OS (Fig. 11d) and IC were negative for this marker. However, stromal myofibroblasts were found in all models, especially in IC (Fig. 12d).

Immunohistochemical Study for Tumor Proliferation

By counting Ki-67 marker-stained cells, the proliferation index of both canine tumor and xenografts was obtained. Values for the primary canine tumor and mean values $\pm$ standard error for xenografts are shown in Table 3. Significant differences ($P < .001$) were found between the 3 models. The IC model had the highest tumor proliferation index followed by CC and OS (Figs. 13a, 14a, 15a). Xenografts had lower proliferation rates than the primary canine tumors from which they came. A significant relationship ($P < .05$) was found between the percentage of Ki-67 and the amount of stroma in both carcinomas and the presence of dermal emboli in the IC model; consequently, tumors with less stroma and the presence of dermal emboli had a higher rate of tumor proliferation.

Immunohistochemical Study of Vascular Factors and COX-2

Expression of factors related to tumor vascularization is shown in Table 4.

VEGF-A immunostaining (Figs. 13b, 14b, 15b) was positive in significantly ($P < .001$) more tumors in the IC model than in the OS model. Positive expression was also higher in the IC model than in the CC model, but it was not significant. Furthermore, in the IC model, increased expression of VEGF-A was associated with a high proliferation index ($P = .048$). VEGF-D expression in the IC model was significantly increased ($P < .001$) compared with CC and OS models (Figs. 13c, 14c, 15c). In the CC model, a significant positive association ($P = .001$) between VEGF-A and VEGF-D was found. Higher expression in IC tumors with dermal emboli ($P = .025$) and with a higher percentage of Ki-67–positive cells ($P < .001$) was observed. VEGFR-3 expression, similar to VEGF-D, was significantly higher ($P < .001$) in the IC model compared with the CC and OS models (Figs. 13d, 14d, 15d). In the CC model, a significant relationship between VEGFR-3 expression and both VEGF-A ($P = .03$) and the Ki-67 index ($P = .04$) was found, indicating that higher expression of VEGFR-3 correlated with higher expression of VEGF-A and the tumor

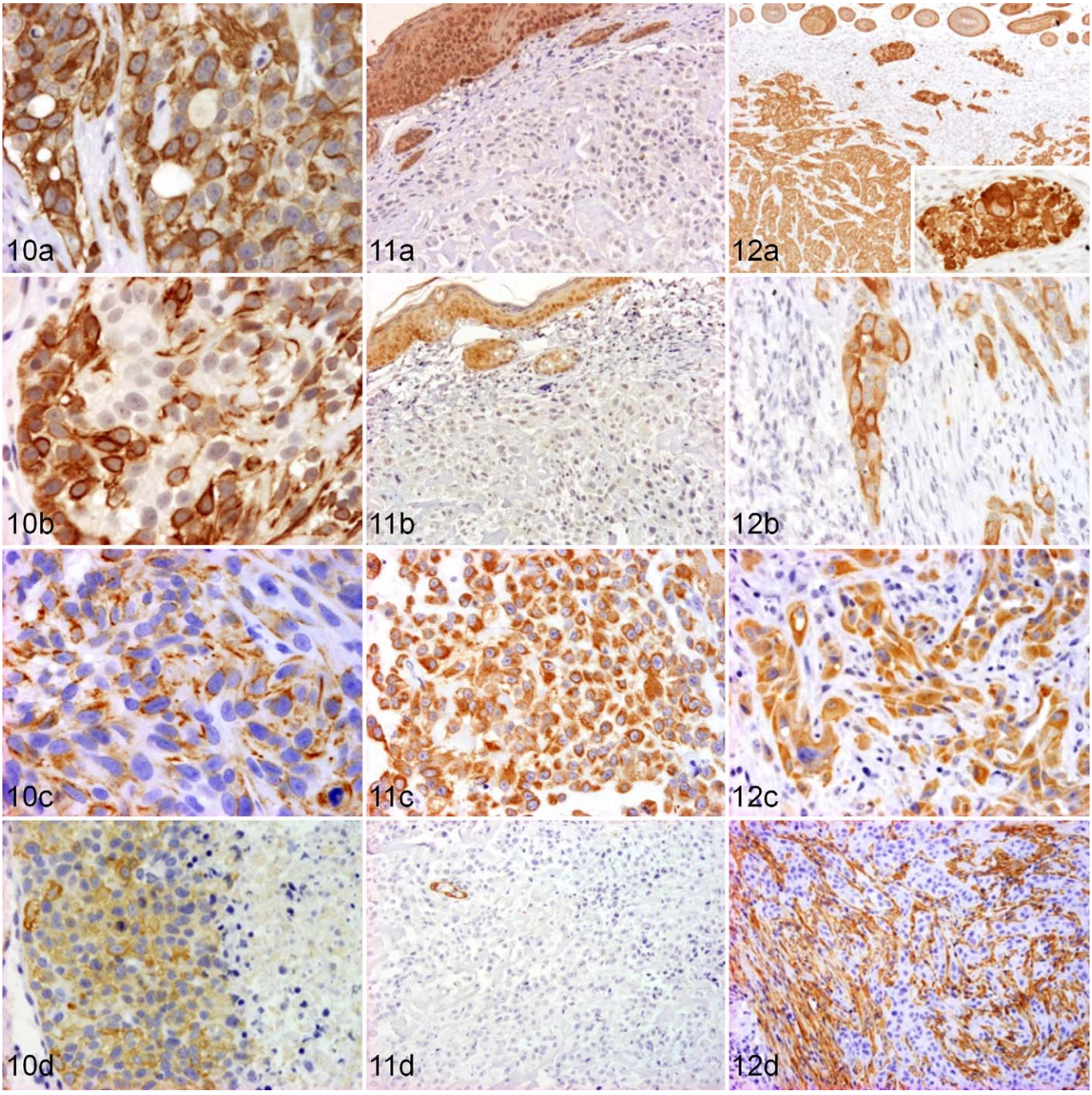

Figure 10. Mammary comedocarcinoma (CC) tumor; SCID (BALB/cJHan^{TM}Hsd-Prkdc^{SCID}) mouse xenograft No. 1. (a) Strongly positive neoplastic cells for pancytokeratin staining. Streptavidin-biotin-peroxidase anti–cytokeratin AE1/AE3, counterstained with hematoxylin. (b) Neoplastic cells show moderate to strong positivity for cytokeratin 14. Streptavidin-biotin-peroxidase anti–cytokeratin 14, counterstained with hematoxylin. (c) Neoplastic cells show a light to moderate expression for vimentin. Streptavidin-biotin-peroxidase antivimentin, counterstained with hematoxylin. (d) Neoplastic cells show moderate or intense positivity for actin. Streptavidin-biotin-peroxidase anti–smooth muscle actin, counterstained with hematoxylin. **Figure 11.** Mammary osteosarcoma (OS) tumor; SCID mouse xenograft No. 2. (a) Neoplastic cells negative for pancytokeratin staining. Streptavidin-biotin-peroxidase anti–cytokeratin AE1/AE3, counterstained with hematoxylin. (b) Neoplastic cells negative for cytokeratin 14. Streptavidin-biotin-peroxidase anti–cytokeratin 14, counterstained with hematoxylin. (c) Neoplastic cells show moderate expression for vimentin. Streptavidin-biotin-peroxidase antivimentin, counterstained with hematoxylin. (d) Neoplastic cells negative for actin. Streptavidin-biotin-peroxidase anti–smooth muscle actin, counterstained with hematoxylin. **Figure 12.** Mammary inflammatory carcinoma (IC) tumor; SCID mouse xenograft No. 3. (a) Neoplastic cells strongly positive for pancytokeratin. Insert showing necrotic tumor cells in an embolus. Streptavidin-biotin-peroxidase anti–cytokeratin AE1/AE3, counterstained with hematoxylin. (b) Neoplastic cells show moderate positivity for cytokeratin 14. Streptavidin-biotin-peroxidase anti–cytokeratin 14, counterstained with hematoxylin. (c) Neoplastic cells show moderate expression for vimentin. Streptavidin-biotin-peroxidase antivimentin, counterstained with hematoxylin. (d) Neoplastic cells negative for actin, with stromal myofibroblasts intensely stained. Streptavidin-biotin-peroxidase anti–smooth muscle actin, counterstained with hematoxylin.

Table 3. Tumor Proliferation Index.

% Ki-67	Comedocarcinoma	Osteosarcoma	Inflammatory Carcinoma
Canine tumor	42	28.8	70
Xenografts (mean ± standard error)	33.8[a] ± 1.7	17.5[b] ± 0.8	44[c] ± 1.4

Superscripted letters denote significant differences ($P < .001$) between the different models.

proliferation index. Once again, increased expression of VEGFR-3 was associated with the presence of dermal emboli ($P = .033$) and a higher Ki-67 index ($P = .03$) in the IC model. COX-2 expression was higher ($P < .001$) in the IC model compared with CC and OS. In general, the primary CC tumor and xenografts were negative for COX-2, but they showed some intensively stained cells located at the edge of necrotic centers, near karyorrhectic areas (Fig. 13e). Immunostaining with apoptosis marker caspase 3 in this model showed positive apoptotic bodies and cells in the necrotic center of comedotype structures. The OS model was also considered negative for COX-2, although it had some moderately positive cells surrounding necrotic areas in both the primary canine tumor and xenografts (Fig. 14e). In the IC model, canine tumor cells and xenografts were heterogeneously positive with moderate or slight intensity (Fig. 15e). COX-2 intensity was also associated with the presence of tumor emboli ($P = .008$) and with VEGFR-3 expression intensity ($P = .027$). Strong positive cells, both isolated and grouped and not necessarily around necrotic areas, were observed and related with increased VEGF-D ($P = .13$) and VEGFR-3 ($P = .023$) expression.

Discussion

This is the first in vivo comparative study of human and canine inflammatory breast carcinoma, with 2 other canine mammary tumors (comedocarcinoma and osteosarcoma), through the development of 3 models in immunocompromised mice. To the best of our knowledge, there are no prior developed animal models for canine mammary comedocarcinoma or canine inflammatory carcinoma. However, 2 human IBC models were developed in mice, MARY-X and WIBC-9.[1,44] A canine mammary osteosarcoma cell line, MCO-Y4, was also developed.[54] Tumor genetic analysis in this study showed that 100% of xenograft genetic content belongs to the canine species. No metastases were observed in xenografts. Relatively few xenografts may reproduce the frequency and distribution of metastases because this is a complex phenomenon that requires special conditions.[6]

The comedocarcinoma model showed comedo structure formation during tumor progression, with necrotic areas in the center of neoplastic cell aggregates. Karyorrhectic residue and apoptotic bodies identified with caspase 3 were observed in these areas. This model confirms that these necrotic centers are formed by a combination of apoptosis and necrosis, as has been described in human CC.[29]

The osteosarcoma model showed a calcified osteoid matrix with necrotic areas increasing with tumor duration. The inflammatory carcinoma model showed typical human and canine IC characteristics.[23,35] The invasion and dilatation of dermal lymphatic vessels by neoplasic emboli and the severe edema histopathologically confirmed the diagnosis based on clinical signs.[17,41]

Both CC and IC models were positive for AE1/AE3, CK14, and vimentin, while actin was only positive in the CC model. Pancytokeratin expression shows the epithelial origin of the neoplasm,[25,30] CK14 recognizes the basal/myoepithelial cells of mammary tumors,[19] and actin stains myoepithelial cells.[52] Vimentin is a marker for mesenchymal origin cells, in both normal and tumoral tissues.[2] According to the tumor phenotype markers, all CC xenografts showed a basal/myoepithelial origin, whereas a basal epithelial origin was observed in IC xenografts. In the OS model, the immunoexpression was typical for sarcoma, with vimentin-positive staining and negative expression for cytokeratins (AE1/AE3 and CK14) and actin. The high malignancy of both carcinoma models is reflected in the coexpression of vimentin and cytokeratin, since it has been suggested that malignant mammary tumors with this phenotype are more aggressive and have a worse prognosis.[50]

In addition to marking myoepithelial cells, actin is used to differentiate the tumor stromal myofibroblasts.[52] Actin expression was observed in all 3 models. It has been proposed that myofibroblasts have a role in tumor cell growth stimulation by the secretion of stromal-derived factor. The presence of myofibroblasts was higher in the IC model, possibly due to its high malignancy. The increased presence of myofibroblasts in canine IC stroma has been shown previously.[8]

Ki-67 antibody is used to determine the rate of tumor proliferation by detecting a nuclear antigen, which is present only in proliferative cells that are in all phases of the cell cycle, but not after mitosis.[15] Breast tumors with a higher histological malignancy grade have a higher tumor proliferation index,[11] and they have been related to a poor prognosis in malignant mammary tumors in both women[47] and dogs.[34] In our study, significant differences were found in the rate of proliferation between the 3 models. As expected, the highest percentage of Ki-67 was found in the IC model since it is considered the most aggressive mammary malignancy with the worst prognosis,[49] followed by the CC model since human CC is the ductal carcinoma in situ with the highest proliferation rate.[27] All xenografts had a lower proliferation index than their primary canine tumors, suggesting a possible loss of proliferative capacity and histological malignancy. In both carcinomas, the proliferation index was lower in tumors with higher amounts of stroma, suggesting that stroma may slow tumor growth, as previously observed.[43] Although the number of tumor emboli is not considered a prognostic factor in patients with IC, this IC model shows that tumors with dermal emboli have a higher proliferation index ($P = .02$).

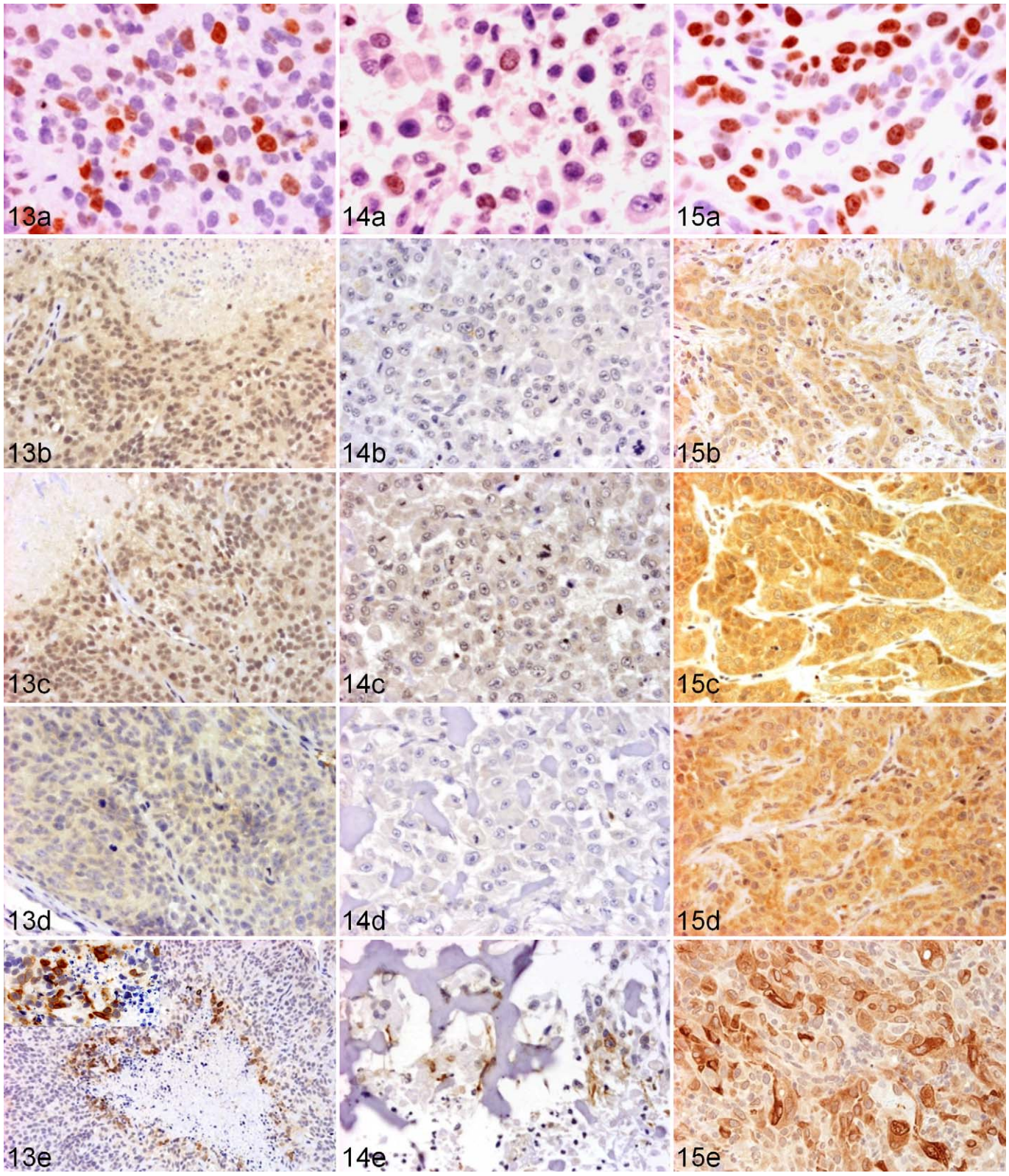

Figure 13. Mammary comedocarcinoma (CC) tumor; SCID (BALB/cJHan^{TM}Hsd-Prkdc^{SCID}) mouse xenograft No. 1. (a) In total, 33.8% of neoplastic cells were positive for Ki-67. Streptavidin-biotin-peroxidase anti–Ki-67, counterstained with hematoxylin. (b) Neoplastic cells show light expression for VEGF-A. Streptavidin-biotin-peroxidase anti–VEGF-A, counterstained with hematoxylin. (c) Neoplastic cells show light positivity for VEGF-D. Streptavidin-biotin-peroxidase anti–VEGF-D, counterstained with hematoxylin. (d) Neoplastic cells show light expression for VEGFR-3. Streptavidin-biotin-peroxidase anti–VEGFR-3, counterstained with hematoxylin. (e) Xenografts negative for COX-2 with neoplastic

Table 4. Immunoexpression of Vascularization Factors in Canine Tumors and Xenografts.

	Comedocarcinoma		Osteosarcoma		Inflammatory Carcinoma	
Factor	Canine Tumor	Xenografts	Canine Tumor	Xenografts	Canine Tumor	Xenografts
VEGF-A	1	0 (46.2) 1 (53.8)	1	0 (84.2) 1 (15.8)	0	0 (29.1) 1 (66.7) 2 (4.2)
VEGF-D	2	1 (45) 2 (55.0)	1	0 (11.8) 1 (58.8) 2 (29.4)	3	2 (66.7) 3 (33.3)
VEGFR-3	1	0 (42.1) 1 (57.9)	1	0 (94.7) 1 (5.3)	2	1 (41.7) 2 (58.3)
COX-2	0	0 (100)	0	0 (100)	2	1 (81) 2 (19)

Immunoexpression was classified into 4 categories (0 to 3), according to the percentage of positive cells and staining intensity. In xenografts, the percentage of tumors corresponding to each intensity is shown in parentheses.

VEGF-A, VEGF-D, and VEGFR-3 showed increased expression in the IC model compared with CC and OS, showing the greater vascularization ability of IC. Higher VEGF-A levels have been found in both canine[8,28] and human IC.[4,44] VEGF-A plays an important role in IC tumor angiogenesis, and it is considered a potential therapeutic target for treatment. VEGF-A inhibitors such as bevacizumab are currently being investigated in patients with IC.[12] Higher expression of VEGF-C, VEGF-D, and VEGFR-3 has also been found in human IBC malignant tumors compared with non-IBC,[53] but there are no previously published reports regarding canine mammary tumors.[8] Similar to VEGF-A, these lymphangiogenic factors and their receptor could be investigated as therapeutic targets for IC, as previously suggested.[18] According to these results, higher VEGF-A expression in CC xenografts correlated with higher VEGF-D and VEGFR-3 expression. The correlation between VEGF-A and VEGF-D was also observed in canine and human mammary tumors.[8,16] Moreover, a correlation between VEGF-D and VEGFR-3 was found in the IC model, which might be related to its lymphangiogenic properties as it was also observed in IMC[8] and IBC.[53] It seems that angiogenic and lymphangiogenic processes are related in CC while the lymphangiogenic process dominates in IC.

In both carcinoma models, the highest tumor proliferation rate was found in tumors with the highest expression of all analyzed vascular factors. A relationship between high VEGF-A expression and a high rate of proliferation was found in human breast tumors and canine IC.[8,13] The relationship between the Ki-67 index and VEGF-D and VEGFR-3 was significant in IC xenografts, while in the CC model, a higher proliferation index was significantly correlated with the VEGFR-3 receptor. These findings indicate that tumor vascularization supports neoplasia development, since tumoral cells can proliferate more with a greater flow of oxygen and nutrients. VEGF-A, VEGF-D, and VEGFR-3 xenograft expression was equal to or less than what was observed in the canine neoplasm. Therefore, a decrease in the angiogenic and lymphangiogenic properties and the rate of cell proliferation showed a loss of malignancy in xenografts compared with the primary canine tumor.

Higher VEGF-D and VEGFR-3 expression was observed in IC with dermal emboli. It has been shown that VEGF increases the microvascular permeability;[14,31] thus, tumors with higher expression of these factors and receptors might stimulate the neoplastic cell migration through tumor lymphatic vessels. Vasculogenic mimicry (VM) was identified in the IC canine tumor and numerous xenografts. VM has been shown to occur more frequently in IC compared with other types of mammary tumors, in both humans[45] and dogs,[7] and it might partially replace the blood vessel function. Moreover, it would be

Figure 13. (continued). cells located at the edge of the necrotic center in comedo structures showing intense expression for COX-2. Insert shows these intensely stained cells in detail. Streptavidin-biotin-peroxidase anti–COX-2, counterstained with hematoxylin. **Figure 14.** Mammary osteosarcoma (OS) tumor; SCID mouse xenograft No. 2. (a) In total, 17.5% of neoplastic cells were positive for Ki-67. Streptavidin-biotin-peroxidase anti–Ki-67, counterstained with hematoxylin. (b) Neoplastic cells show light expression for VEGF-A. Streptavidin-biotin-peroxidase anti–VEGF-A, counterstained with hematoxylin. (c) Neoplastic cells show light positivity for VEGF-D. Streptavidin-biotin-peroxidase anti–VEGF-D, counterstained with hematoxylin. (d) Neoplastic cells show negative expression for VEGFR-3. Streptavidin-biotin-peroxidase anti–VEGFR-3, counterstained with hematoxylin. (e) Xenografts negative for COX-2 with some cells surrounding necrotic areas were moderately positive. Streptavidin-biotin-peroxidase anti–COX-2, counterstained with hematoxylin. **Figure 15.** Mammary inflammatory carcinoma (IC) tumor; SCID mouse xenograft No. 3. (a) In total, 44% of neoplastic cells were positive for Ki-67. Streptavidin-biotin-peroxidase anti–Ki-67, counterstained with hematoxylin. (b) Neoplastic cells show moderate expression for VEGF-A. Streptavidin-biotin-peroxidase anti–VEGF-A, counterstained with hematoxylin. (c) Neoplastic cells show intense positivity for VEGF-D. Streptavidin-biotin-peroxidase anti–VEGF-D, counterstained with hematoxylin. (d) Neoplastic cells show moderate expression for VEGFR-3. Streptavidin-biotin-peroxidase anti–VEGFR-3, counterstained with hematoxylin. (e) Neoplastic cells show moderate expression for COX-2 with groups of intensely stained cells. Streptavidin-biotin-peroxidase anti–COX-2, counterstained with hematoxylin.

closely related to the lymphatic circulation and may be another mechanism of disease dissemination.[20]

It has been shown that COX-2 plays a role in the invasive and angiogenic phenotype of IC.[40,53] IC xenografts had a low or moderate heterogeneous positivity for COX-2, with some isolated and grouped strongly positive cells, while CC and OS models showed negative expression. Other authors have found higher levels of this molecule in canine IC tumors compared with non-IC mammary tumors, suggesting a special role for COX-2 in extracellular matrix degradation and lymphangiogenic pathway stimulation.[8,38] In the current IC model, COX-2 expression was also related to the presence of tumor emboli in lymphatic vessels within the tumor, suggesting that this molecule could stimulate formation of these emboli, since COX-2 favors tumoral extravasation and distant metastases.[32]

The presence of cells with high COX-2 expression was associated with increased VEGF-D ($P = .013$) and VEGFR-3 ($P = .023$) expression in the IC model. A significant correlation between COX-2 and angiogenic factors such as VEGF-A[10,39] and lymphangiogenic factors such as VEGF-C[51] has been shown in both human and canine mammary tumors, suggesting that COX-2 modulates the release of these angiogenic and lymphangiogenic factors. In a previous study,[8] COX-2 expression was associated with VEGF-A in malignant non-IC mammary tumors, while it was associated with VEGF-D in IC tumors. According to these results, it is possible that angiogenic and lymphangiogenic mechanisms are different in both tumor groups, with the lymphangiogenic process in IC being COX-2 related.

The ability of COX-2 to suppress apoptosis has been studied. It has been shown that a decrease in the apoptosis level promotes carcinogenesis by allowing the survival of cells that have acquired mutations.[21] In the CC model, although all the tumors were considered negative for COX-2 expression, some COX-2 intensively positive cells were found repeatedly at the boundary of the comedo-type structures along the necrotic center. This finding suggests that COX-2 is involved in the apoptosis of the comedo structures. This role for COX-2 has not been previously studied in either human or canine mammary comedocarcinoma. Surprisingly, some COX-2–positive cells around the necrotic areas in the OS model were also observed.

In conclusion, inflammatory mammary carcinoma xenografts showed the highest vascular factor expression compared with osteosarcoma and comedocarcinoma and were associated with a high proliferation index. Likewise, IC xenografts showed higher COX-2 expression associated with VEGF-D, VEGFR-3, and the presence of lymphatic tumor emboli, suggesting COX-2 participation in IC lymphangiogenesis. These results show more evidence to consider the vascular factors, their receptors, and COX-2 as therapeutic targets for both IBC and IMC. However, due to the small number of samples used to develop the xenografts, more studies are required. In addition, the CC model shows that necrotic areas of comedo-type formation are a mixture of necrosis and apoptosis in which COX-2 has an important role, probably via apoptosis.

Acknowledgements

We are grateful to M[a] Dolores Pérez Alenza for the referred cases; Pedro Cuesta, from the Complutense University Processing Data Center, for his assistance with the statistical work; and Pedro Aranda for his histotechnology assistance.

Declaration of Conflicting Interests

The author(s) declared no potential conflicts of interest with respect to the research, authorship, and/or publication of this article.

Funding

The author(s) disclosed receipt of the following financial support for the research, authorship and/or publication of this article: This work was supported by the Spanish Ministry of Science and Education (research project No. SAF 2009-10572 and PhD fellowship).

References

1. Alpaugh ML, Tomlinson JS, Shao ZM, et al. A novel human xenograft model of inflammatory breast cancer. *Cancer Res*. 1999;**59**(20):5079–5084.
2. Azumi N, Battifora H. The distribution of vimentin and keratin in epithelial and nonepithelial neoplasms: a comprehensive immunohistochemical study on formalin- and alcohol-fixed tumors. *Am J Clin Pathol*. 1987;**88**:286–296.
3. Basu GD, Liang WS, Stephan DA, et al. A novel role for cyclooxygenase-2 in regulating vascular channel formation by human breast cancer cells. *Breast Cancer Res*. 2006;**8**(6):R69.
4. Bièche I, Lerebours F, Tozlu S, et al. Molecular profiling of inflammatory breast cancer: identification of a poor-prognosis gene expression signature. *Clin Cancer Res*. 2004;**10**(20): 6789–6795.
5. Chang SH, Liu CH, Conway R, et al. Role of prostaglandin E2-dependent angiogenic switch in cyclooxygenase 2–induced breast cancer progression. *Proc Natl Acad Sci U S A*. 2004; **101**(2):591–596.
6. Clarke R, Haier J. *Human Tumours in Animal Hosts: The Cancer Handbook*. New York, NY: John Wiley; 2007.
7. Clemente M, Pérez-Alenza MD, Illera JC, et al. Histological, immunohistological and ultrastructural description of vasculogenic mimicry in canine mammary cancer. *Vet Pathol*. 2010; **47**(2):265–274.
8. Clemente M, Sánchez-Archidona AR, Sardon D, et al. Different role of COX-2 and angiogenesis in canine inflammatory and non-inflammatory mammary cancer. *Vet J*. 2013;**197**(2): 427–432.
9. Colpaert CG, Vermeulen PB, Benoy I, et al. Inflammatory breast cancer shows angiogenesis with high endothelial proliferation rate and strong E-cadherin expression. *Br J Cancer*. 2003;**88**(5): 718–725.
10. Costa C, Soares R, Reis-Filho JS, et al. Cyclo-oxygenase 2 expression is associated with angiogenesis and lymph node metastasis in human breast cancer. *J Clin Pathol*. 2002;**55**: 429–434.
11. Crispino S, Brenna A, Colombo D, et al. Ki-67 labeling index in breast cancer. *Tumori*. 1989;**75**(6):557–562.

12. Dawood S, Cristofanilli M. Inflammatory breast cancer: what progress have we made? *Oncology (Williston Park)*. 2011; **25**(3):264–270.
13. Fuckar D, Dekanic A, Stifter S, et al. VEGF expression is associated with negative estrogen receptor status in patients with breast cancer. *Int J Surg Pathol*. 2006;**14**(1):49–55.
14. Gasparini G. Prognostic value of vascular endothelial growth factor in breast cancer. *Oncologist*. 2000;**5**(suppl 1):37–44.
15. Gerdes J, Lemke H, Baisch H, et al. Cell cycle analysis of a cell proliferation-associated human nuclear antigen defined by the monoclonal antibody Ki-67. *J Immunol*. 1984;**133**(4):1710–1715.
16. Gisterek I, Matkowski R, Lacko A, et al. Serum vascular endothelial growth factors a, C and d in human breast tumors. *Pathol Oncol Res.* 2010;**16**(3):337–344.
17. Goldschmidt M, Peña L, Rasotto R, et al. Classification and grading of canine mammary tumors. *Vet Pathol*. 2011;**48**(1): 117–131.
18. Gong Y. Pathologic aspects of inflammatory breast cancer, part 2: biologic insights into its aggressive phenotype. *Semin Oncol*. 2008;**35**(1):33–40.
19. Griffey SM, Madewell BR, Dairkee SH, et al. Immunohistochemical reactivity of basal and luminal epithelium-specific cytokeratin antibodies within normal and neoplastic canine mammary glands. *Vet Pathol*. 1993;**30**:155–161.
20. Hendrix MJ, Seftor EA, Hess AR, et al. Vasculogenic mimicry and tumour-cell plasticity: lessons from melanoma. *Nat Rev Cancer*. 2003;**3**(6):411–421.
21. Howe LR, Subbaramaiah K, Brown AM, et al. Cyclooxygenase-2: a target for the prevention and treatment of breast cancer [review]. *Endocr Relat Cancer*. 2001;**8**(2):97–114.
22. Hsu SM, Raine L, Fanger H. Use of avidin-biotin-peroxidase complex (ABC) in immunoperoxidase techniques: a comparison between ABC and unlabeled antibody (PAP) procedures. *J Histochem Cytochem*. 1981;**29**(4):577–580.
23. Kleer CG, van Golen KL, Merajver SD. Molecular biology of breast cancer metastasis. Inflammatory breast cancer: clinical syndrome and molecular determinants. *Breast Cancer Res*. 2000;**2**(6):423–429.
24. Langenbach A, Anderson MA, Dambach DM, et al. Extraskeletal osteosarcomas in dogs: a retrospective study of 169 cases (1986–1996). *J Am Anim Hosp Assoc*. 1998;**34**:113–120.
25. Listrom MB, Dalton LW. Comparison of keratin monoclonal antibodies MAK-6, AE1: AE3, and CAM-5.2. *Am J Clin Pathol*. 1987;**88**:297–301.
26. Maniotis AJ, Folberg R, Hess A, et al. Vascular channel formation by human melanoma cells in vivo and in vitro: vasculogenic mimicry. *Am J Pathol*. 1999;**155**(3):739–752.
27. Meyer J. Cell kinetics of histologic variants of in situ breast carcinoma. *Breast Cancer Res Treat*. 1986;**7**:171–180.
28. Millanta F, Caneschi V, Ressel L, et al. Expression of vascular endothelial growth factor in canine inflammatory and non-inflammatory mammary carcinoma. *J Comp Pathol*. 2010; **142**(1):36–42.
29. Moinfar F, Mannion C, Man YG, et al. Mammary ''comedo''-DCIS: apoptosis, oncosis, and necrosis: an electron microscopic examination of 8 cases. *Ultrastruct Pathol*. 2000;**24**(3):135–144.
30. Mygind H, Nielsen B, Moe D, et al. Antikeratin antibodies in routine diagnostic pathology: a comparison of 10 different commercial antikeratins. *APMIS*. 1988;**96**:1009–1022.
31. Nakamura J, Savinvov A, Lu Q, et al. Estrogen regulates vascular endothelial growth/permeability factor expression in 7,12-dimethylbenz(a)anthracene-induced rat mammary tumors. *Endocrinology*. 1996;**137**(12):5589–5596.
32. Nguyen DX, Bos PD, Massague J. Metastasis: from dissemination to organ-specific colonization. *Nat Rev Cancer*. 2009;**9**(4): 274–284.
33. Nieto A, Peña L, Pérez-Alenza MD, et al. Immunohistologic detection of estrogen receptor alpha in canine mammary tumors: clinical and pathologic associations and prognostic significance. *Vet Pathol*. 2000;**37**(3):239–247.
34. Peña L, Nieto AI, Pérez-Alenza D, et al. Immunohistochemical detection of Ki-67 and PCNA in canine mammary tumors: relationship to clinical and pathologic variables. *J Vet Diagn Invest*. 1998;**10**(3):237–246.
35. Peña L, Pérez-Alenza MD, Rodríguez-Bertos A, et al. Canine inflammatory mammary carcinoma: histopathology, immunohistochemistry and clinical implications of 21 cases. *Breast Cancer Res Treat*. 2003;**78**(2):141–148.
36. Pérez-Alenza MD, Tabanera E, Peña L. Inflammatory mammary carcinoma in dogs: 33 cases (1995–1999). *J Am Vet Med Assoc*. 2001;**219**(8):1110–1114.
37. Prosperi JR, Mallery SR, Kigerl KA, et al. Invasive and angiogenic phenotype of MCF-7 human breast tumor cells expressing human cyclooxygenase-2. *Prostaglandins Other Lipid Mediat*. 2004;**73**:249–264.
38. Queiroga FL, Pérez-Alenza MD, Silván G, et al. Cox-2 levels in canine mammary tumors, including inflammatory mammary carcinoma: clinicopathological features and prognostic significance. *Anticancer Res*. 2005;**25**(6B):4269–4275.
39. Queiroga FL, Raposo T, Carvalho MI, et al. Canine mammary tumours as a model to study human breast cancer: most recent findings. *In Vivo*. 2011;**25**(3):455–465.
40. Robertson FM, Simeone AM, Mazumdar A, et al. Molecular and pharmacological blockade of the EP4 receptor selectively inhibits both proliferation and invasion of human inflammatory breast cancer cells. *J Exp Ther Oncol*. 2008;**7**(4):299–312.
41. Robertson FM, Bondy M, Yang W, et al. Inflammatory breast cancer: the disease, the biology, the treatment. *CA Cancer J Clin*. 2010;**60**(6):351–375.
42. Sambrook J, Fritsch EF, Maniatis T. *Molecular Cloning: A Laboratory Manual*. 2nd ed. New York, NY: Cold Spring Harbor Laboratory Press; 1989.
43. Seemayer TA, Lagacé R, Schürch W, et al. Myofibroblasts in the stroma of invasive and metastatic carcinoma: a possible host response to neoplasia. *Am J Surg Pathol*. 1979;**3**(6):525–533.
44. Shirakawa K, Tsuda H, Heike Y, et al. Absence of endothelial cells, central necrosis, and fibrosis are associated with aggressive inflammatory breast cancer. *Cancer Res*. 2001;**61**(2): 445–451.
45. Shirakawa K, Wakasugi H, Heike Y, et al. Vasculogenic mimicry and pseudo-comedo formation in breast cancer. *Int J Cancer*. 2002;**99**(6):821–828.

46. Silverstein MJ, Lagios MD, Craig PH, et al. A prognostic index for ductal carcinoma in situ of the breast. *Cancer*. 1996;**77**(11): 2267–2274.
47. Stuart-Harris R, Caldas C, Pinder SE, et al. Proliferation markers and survival in early breast cancer: a systematic review and meta-analysis of 85 studies in 32,825 patients. *Breast*. 2008;**17**(4): 323–334.
48. Susaneck SJ, Allen TA, Hoopes J, et al. Inflammatory mammary carcinoma in the dog. *J Am Anim Hosp Assoc*. 1983;**9**:971–976.
49. Tavassoli FA. *Pathology of the Breast*. 2nd ed. New York, NY: McGraw-Hill; 1999.
50. Thomas PA, Kirschmann DA, Cerhan JR, et al. Association between keratin and vimentin expression, malignant phenotype, and survival in postmenopausal breast cancer patients. *Clin Cancer Res*. 1999;**5**(10):2698–2703.
51. Timoshenko AV, Chakraborty C, Wagner GF, et al. COX-2–mediated stimulation of the lymphangiogenic factor VEGF-C in human breast cancer. *Br J Cancer*. 2006;**94**:1154–1163.
52. Tsukada T, McNutt MA, Ross R, et al. HHF35, a muscle actin-specific monoclonal antibody, II: reactivity in normal, reactive, and neoplastic human tissues. *Am J Pathol.* 1987;**127**(2): 389–402.
53. Van der Auwera I, Van Laere SJ, Van den Eynden GG, et al. Increased angiogenesis and lymphangiogenesis in inflammatory versus non inflammatory breast cancer by real-time reverse transcriptase-PCR gene expression quantification. *Clin Cancer Res*. 2004;**10**(23):7965–7971.
54. Wensman H, Flama V, Pejler G , et al. Plasticity of cloned canine mammary spindle cell tumor, osteosarcoma and carcinoma cells. *Vet Pathol*. 2008;**45**(6):803–815.